Lasers Med Sci
DOI 10.1007/s10103-011-0976-0

ORIGINAL ARTICLE

Influence of creatine supplementation on bone quality in the ovariectomized rat model: an FT-Raman spectroscopy study

Renato Aparecido de Souza · Murilo Xavier · Fabiano Fernandes da Silva · Marco Túlio de Souza · Maira Gaspar Tosato · Airton Abrahão Martin · Julio Cezar de Melo Castilho · Wellington Ribeiro · Landulfo Silveira Jr.

Received: 28 April 2011 / Accepted: 15 July 2011

Abstract The influence of creatine (Cr) supplementation on cortical and trabecular bone from ovariectomized rats was studied using FT-Raman spectroscopy. The intensity of organic-phase Raman bands was compared to mineral phase ones. Twenty-one female Wistar rats aged 3 months were divided into three groups (n=7 per group): ovariectomized (OVX), ovariectomized treated with creatine (CRE) and sham-operated (SHAM) groups. Creatine supplementation (300 mg kg^{-1} day^{-1}) was provided for 8 weeks, starting 12 weeks after ovariectomy. FT-Raman spectroscopy was performed on the right medial femoral mid-shaft (cortical bone) and third lumbar vertebral body (trabecular bone). The integrated intensities of mineral phase (phosphate and carbonate bands at 959 and 1,071 cm^{-1}, respectively) and organic phase (amide I band at 1,665 cm^{-1}) Raman bands were analyzed. The mineral-to-matrix (phosphate/amide I), carbonate-to-phosphate, and carbonate-to-amide I ratios were analyzed to assess bone quality. The phosphate content on trabecular bone was higher in the CRE group than the OVX group ($p<0.05$). No significant changes in mineral or organic phases on cortical bone were observed. A radiographic assessment of bone density was encouraging as the same findings were showed by Raman intensity of phosphate from cortical (r^2=0.8037) and trabecular bones (r^2=0.915). Severe ovariectomy-induced bone loss was confirmed by FT-Raman spectroscopy. The results suggest that the chemical composition of trabecular bone tissue may be positively influenced by Cr supplementation after ovariectomy.

Keywords Cortical bone · Nutritional supplement · Optical spectroscopy · Osteoporosis · Trabecular bone

Introduction

Creatine (Cr) is a naturally occurring amino acid-like compound obtained by the synthesis of the essential amino

R. A. de Souza (✉) · F. F. da Silva
Grupo de Estudos e Pesquisa em Ciências da Saúde,
Instituto Federal de Educação, Ciência e Tecnologia
do Sul de Minas Gerais,
Muzambinho, MG, Brazil
e-mail: tatosouza2004@yahoo.com.br

M. Xavier
Department of Physical Therapy, Vales do Jequitinhonha e Mucuri
Federal University,
Diamantina, MG, Brazil

M. Xavier · L. Silveira Jr.
Biomedical Engineering Center, Universidade Camilo
Castelo Branco,
São José dos Campos, SP, Brazil

M. T. de Souza
Faculty of Medicine, Vale do Sapucaí University,
Pouso Alegre, MG, Brazil

M. G. Tosato · A. A. Martin
Laboratory of Biomedical Vibrational Spectroscopy, Institute
of Research and Development, Vale do Paraíba University,
São José dos Campos, SP, Brazil

J. C. de Melo Castilho
Departamento de Radiologia, Universidade Estadual Paulista,
São José dos Campos, SP, Brazil

W. Ribeiro
Laboratory of Physiology and Pharmacodynamics, Institute
of Research and Development, Vale do Paraiba University,
São José dos Campos, SP, Brazil

Published online: 12 August 2011

acids arginine, glycine, and methionine in the liver, kidneys, and pancreas (approximately 1–2 g per day), and its major external source is from ingested food (approximately 1–5 g per day), especially from meat and fish [1]. Physiologically, Cr is predominantly used by tissues with high energy demands and it plays an important role in rapid energy provision [2]. Considering that 95% of all Cr is found in skeletal muscle, Cr research has primarily focused on its effects during muscle contraction, by regenerating ATP through a reversible reaction catalyzed by creatine kinase (CK) [3]. Considering the beneficial effects observed from the use of Cr in sports, several studies have investigated the potential use of Cr as a clinical therapeutic agent. Recently, Gualano et al. [4] reviewed the main studies that have been conducted in this field and summarized the scientific and clinical perspectives of this promising therapeutic supplement. There is some evidence to indicate that Cr supplementation is capable of attenuating the degenerative state in some muscle disorders (i.e., Duchenne muscular dystrophy and inflammatory myopathies), central nervous diseases (i.e., Parkinson's, Huntington's, and Alzheimer's diseases), and bone and metabolic disturbances (i.e., osteoporosis and type II diabetes). However, the repercussions of Cr supplementation in individuals suffering from metabolic bone disorder are far less clear.

Osteoporosis is the most common metabolic bone disorder characterized by the progressive loss of bone mass and the microarchitecture deterioration of bone tissue, predisposing patients to an increased risk of bone fractures [5, 6]. The preliminary evidence to show that Cr supplementation could improve bone mass was obtained by Louis et al. [7] with dystrophic patients under chronic corticoid treatment. These authors found that patients with Duchenne dystrophy who were supplemented with Cr showed symptomatic benefits, with a remarkable increase in bone mineral density (BMD) and a reduction in the urinary excretion of bone resorption markers. Some studies assessed the effects of Cr supplementation on BMD in elderly people, who are more likely to suffer from osteoporosis. In general, these studies investigated Cr supplementation combined with resistance training on BMD and concluded that Cr supplementation exerts a beneficial additive effect to resistance training on bone mass [8–10]. However, no data in the literature were found to support a correlation between Cr supplementation and beneficial effects on bone osteoporosis.

Currently, the determination of BMD by dual-energy X-ray absorptiometry (DXA) is considered as the gold-standard screening method for the diagnosis of osteoporosis in humans, identifying the risk of fracture [11]. However, it is interesting to note that bone is a composite biogenic tissue, and since the quality of bone critically depends on both organic (primarily collagen I) and mineral (calcium carbonate and hydroxyl apatites) phases, and since the organic phase remains essentially transparent in X-rays, there is a need for a technique that, in addition to measuring the bone mineral, could assess the collagen in the bone matrix. In fact, the determination of BMD by DXA can account for 60–70% of the variation in bone strength and is only a moderate predictor of fracture risk [12].

In recent years, vibrational spectroscopy such as Fourier-transform Raman spectroscopy (FT-Raman) has been evaluated as a technique for studying "bone quality" [13, 14]. Bone quality refers to the group of compositional and architectural properties of bone tissue that together determine its properties and mechanical functions [15]. Since Raman spectroscopy measures the characteristic vibrational frequencies of molecules, it provides information on the composition of organic and inorganic samples, allowing nondestructive qualitative and quantitative analyses [16, 17]. In this sense, Raman spectroscopy could assess the chemical composition of bone tissue and thus evaluate at least three of the parameters that are important for bone composition and quality, namely, the mineral-to-matrix ratio (phosphate/amide I), which indicates the degree of mineralization, the carbonate-to-phosphate ratio, which varies with bone architecture, age, and mineral crystallinity, and the carbonate-to-amide I ratio, which may indicate bone remodeling [14].

The present study aimed to investigate the influence of Cr supplementation on cortical and trabecular bone from ovariectomized rats, a well-established model for experimental osteoporosis in rats, using the spectral information provided by FT-Raman spectroscopy. This study attempted to elucidate the effects of Cr supplementation on the bone parameters (quality and Raman spectral features) of osteoporotic bone. In addition, the Raman bands of the mineral phase were compared to the radiographic assessment of BMD in order to validate the Raman technique as being a possible bone mineralization quantification tool.

Materials and methods

Animal care and study protocol

This study was conducted according to the Ethical Principles on Animal Experimentation adopted by the Brazilian College of Animal Experimentation (COBEA) and was approved by the Committee for Ethics in Research of the Universidade do Vale do Paraíba (Protocol no. A37/CEP/2008). Thirty female Wistar rats (*Rattus norvegicus*) weighing 225±25 g were obtained from the Bem-Te-Vi Farm (Paulínia, SP, Brazil), at about 80 days of age, and allowed to acclimate for 2 weeks in the bioterium of the Physiology and Pharmacodynamics Laboratory (IP&D, UNIVAP, São José dos Campos. SP, Brazil).

At 3 months of age (where rats reach skeletal maturation), the animals were weight-matched into two groups: the first group was composed of ovariectomized rats (OVX group, n=20), and the second group was submitted to a sham-operation (SHAM group) for the simulation of surgical stress (control, n=10). Each ovariectomy was performed under general anesthesia (10 mg/kg 2% xylazine hydrochloride (Rompun, Bayer, São Paulo, SP, Brazil) and 80 mg/kg ketamine hydrochloride (Francotar, Virbac, Roseira, SP, Brazil)) via two dorso-lateral incisions, approximately 1 cm long, below the last ribs and above the ovaries. With the use of sharp dissecting scissors, the skin was cut, together with the dorsal muscles, the peritoneal cavity was accessed, and thus the ovaries were reached. In the OVX group, hemostasis was performed by ligation of the upper part of the Fallopian tube with a #4.0 catgut suture and the ovaries were excised together with the surrounding fat, the oviduct, and a small portion of the uterus. The muscular incision required no further suturing. Skin wounds were closed bilaterally with a #4.0 silk suture. In the SHAM group, the ovaries were exposed but not removed. After the surgical procedures, all animals were housed in pairs in standard cages in a room maintained at 22±3°C with 12-h light/dark cycles and left untreated for 12 weeks to induce osteoporosis in the OVX groups [18]. At the end of this period, three rats of the SHAM group and six rats of the OVX group were killed in order to evaluate the reduction of bone mass induced by ovariectomy.

Twelve weeks after surgery, the remaining animals (n=21) were again weight-matched into the three experimental groups: rats with osteoporosis (OVX, n=7), rats with osteoporosis and Cr-supplemented for 8 weeks (CRE, n=7), and sham-operated rats (SHAM, n=7). All animals had access to water and food ad libitum (standard laboratory diet, Labcil®, Nutri Forte, Uberaba, MG, Brazil).

Creatine supplementation

The CRE group was fed with micronized creatine (Integral Médica, Embu-Guaçu, SP, Brazil) via esophageal gavage at a dose of 300 mg kg^{-1} of body weight, daily, for 8 weeks. This dose of Cr was used in previous animal studies [19–21] and is equivalent to the customary loading dose of 20 g. day^{-1} in a 70-kg person, which produces maximum effects in 5 days [22, 23]. This dosage regimen was started after only 12 weeks (the period of osteoporosis induction) and the doses were given in the afternoon.

Specimen preparation

All rats were anesthetized with an intramuscular administration of 40 mg.kg^{-1} xylazine HCl (Xilazin 2%, 50 ml; Syntec do Brazil Ltda., São Paulo, Brazil) and 50 mg.kg^{-1} ketamine HCl (Cetamin 10%, 50 ml; Syntec do Brazil Ltda.) and euthanized with an intracardiac injection of KCl solution (Cloreto de potássio 10%; Laboratório Ariston Ltda., São Paulo, Brazil). The right femur and third lumbar vertebra bones were harvested, the soft tissues were cleaned out, and the bones were stored at −89°C in a freezer until analysis. In order to evaluate alterations in the cortical and trabecular bones, the medial femoral mid-shaft and the third lumbar vertebral body were assessed, respectively [24] (Fig. 1). Prior to FT-Raman or radiographic assessments of the BMD experiments, the bones of interest were gradually warmed to room temperature and their surfaces were adequately positioned in the Raman spectrometer and the following the X-ray equipment without any chemical fixation or treatment (i.e., cuts).

FT-Raman spectroscopy analysis

An FT-Raman spectrometer (RFS 100/S®-Bruker, Inc., Karlsruhe, Germany) was used to collect the data. This spectrometer uses an air-cooled Nd:YAG laser (λ= 1,064 nm) for excitation and a liquid N_2-cooled germanium detector. The Nd:YAG laser had an incident power of about 180 mW at the surface of the samples. The spectral resolution was set to 4 cm^{-1} with the use of 200 scans per spectrum. At each bone region of interest (Fig. 1), three spectra were collected with an approximate 10 μm distance between each collection point. Before spectra pre-processing, these three spectra per site of interest were averaged, resulting in a dataset composed of 60 spectra (cortical and trabecular bones of 30 animals measured). Data collection and transfer were automated using the Bruker OPUS™ software. To remove the fluorescence background from the gross spectrum, a fourth-order

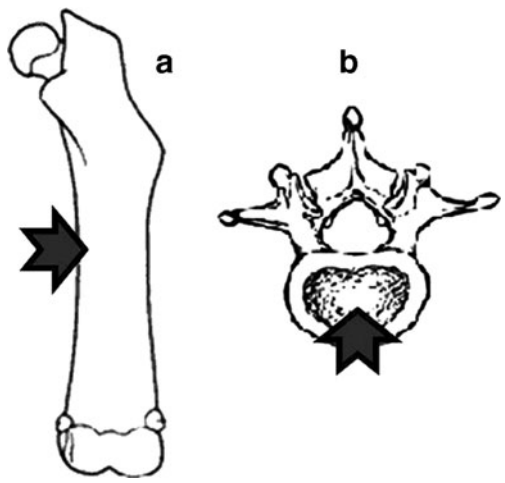

Fig. 1 Measurement positions (*arrows*) used for acquisition of Raman spectra and bone density: **a** medial femoral mid-shaft representing cortical bone; **b** third lumbar vertebral body representing trabecular bone

polynomial fitting was adjusted to each spectrum in the 800–1,800 cm^{-1} region and subtracted. This procedure was routinely performed using Matlab 6.0® software (Newark, NJ, USA).

The spectra were then plotted and the spectral parameters related to bone changes were calculated using Microcal Origin5.0® software (Microcal Software, Inc., Northampton, MA, USA). Integrated intensities of the Raman bands in the intervals: 957–962 cm^{-1} (phosphate) and 1,065–1,071 cm^{-1} (carbonate), representing the mineral content, and 1,595–1,720 cm^{-1} (amide I), representing the organic matrix (collagen) were analyzed to characterize bone changes in the mineral and organic phases [13, 14, 24, 25]. Bone quality was analyzed using the following spectral parameters: (i) ratios of these areas, resulting in measurements of the mineral-to-matrix ratio (phosphate/amide I), which indicates the degree of mineralization [26], (ii) the carbonate-to-phosphate ratio, which varies with bone architecture, age, and mineral crystallinity [27–29], and (iii) the carbonate-to-amide I ratio, which may indicate bone remodeling [26].

Radiographic assessment of bone density

In order to correlate the Raman measurements, the BMD was measured from digital radiographs [30] (image resolution/sharpness: 22.7 lp/mm; image size: 1,368×912 pixels; pixel size: 22×22 μm) taken using a CMOS CCD digital X-ray camera (Visualix GX-S-HDI™, Gendex Dental Systems, Des Plaines, IL, USA). First, the CCD and bone samples were stabilized in a standard fixing device. Following this, each femur was radiographed using X-ray equipment (Spectro-70X™; Dabi Atlante, São Paulo, Brazil) at 10 mA and 65 kVp, with a 0.1 s exposure time and 40 cm focus-object distance. Radiographs were taken from cortical and trabecular bones, and the digital images acquired were transferred to the computer. The images were stored in a TIFF format without compression, with a resolution of 600 dpi. The BMD was evaluated using a gray-level histogram in an area of 5×5 pixels for all bones using the VixWin™ 1.4 software (Gendex Dental Systems, Inc.). All results were expressed in 8-bit gray levels (0–255) [31].

Statistical analysis

The spectral parameters and BMD results are presented as means and standard deviations. Student's *t* tests were used to compare changes among the OVX and SHAM groups prior to Cr supplementation (significance level of 5%). One-way analysis of variance (ANOVA) was used to compare changes among the groups post-Cr supplementation (significance level of 5%). A post-hoc analysis (Tukey-Kramer test) was used to determine the localization of significant differences when necessary. Furthermore, Pearson's correlation coefficient was calculated to correlate the main Raman marker of the bone mineral findings (phosphate band centered at 959 cm^{-1}) with the BMD.

Statistical evaluations (Student's *t* tests and ANOVA tests) of the integrated intensities of the carbonate, phosphate, and amide I bands, the ratios of these bands, and the BMD were analyzed using SPSS software version 11.0 (SPSS Inc, Chicago, IL, USA).

Results

Prior to creatine supplementation (induction of osteoporosis)

Figure 2 presents the BMD of cortical and trabecular bones for the OVX and SHAM groups 12 weeks after ovariectomy, prior to Cr supplementation. In the medial femoral mid-shaft (cortical bone), there was no statistically significant difference between the groups prior to Cr supplementation ($p=0.86$). However, a statistically significant reduction of about 25% of the bone density was observed in the third lumbar vertebral body (trabecular bone) ($p<0.05$). This result confirmed the induction of osteoporosis before Cr supplementation.

Figure 3 presents the Raman spectra of the third lumbar vertebral body from the SHAM and OVX groups, evidencing important differences between the two groups. These spectra showed that both bones had the same peak positions, but the intensities at specific Raman shifts were different. Also, the main Raman bands of the bone tissues at 959, 1,071 and 1,665 cm^{-1} were consistent with previous results [24, 25]. In the bone spectrum, the band centered at 959 cm^{-1} corresponds to the symmetric stretching vibration of primary phosphate (PO_4^{3-}) and it is the strongest bone

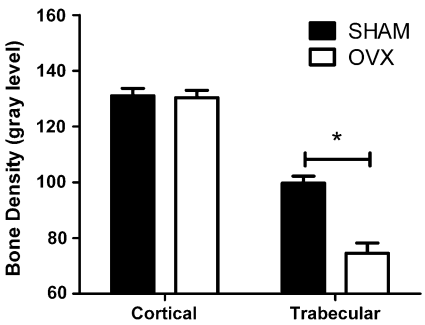

Fig. 2 Means and standard deviations of radiographic BMD of the animals who received bilateral ovariectomy (OVX, $n=6$) and a sham operation (SHAM, $n=3$) 12 weeks after surgery, before Cr supplementation; *indicates the OVX group with a statistically significant difference compared to the SHAM group for same bone region ($p<0.05$)

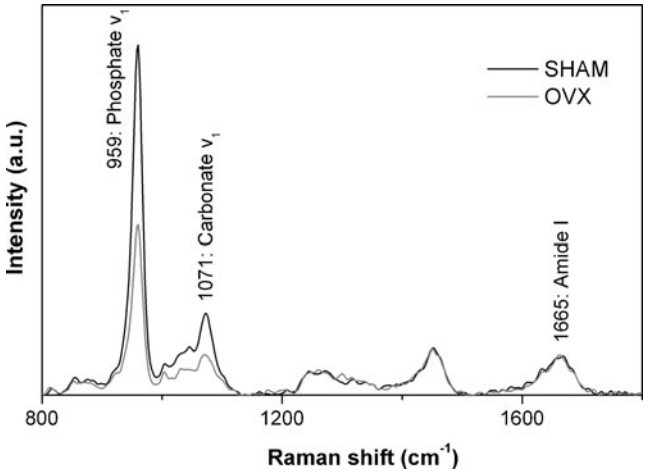

Fig. 3 Typical FT-Raman spectra from the third lumbar vertebral body of OVX (*gray line*) and SHAM (*black line*) animals showing the major peaks and their molecular constituents. Raman bands at 959 cm^{-1} and 1,071 cm^{-1} represent the bone mineral content and the Raman band at 1,665 cm^{-1} represents the organic matrix from collagen content; *a.u.* arbitrary units

mineral marker. The peak at 1,071 cm^{-1} corresponds to the stretching vibrational mode of primary carbonate (CO_3^{2-}) and indicates the extent of carbonate incorporation in the hydroxyapatite lattice (type-B carbonate substitution). The main Raman band of the organic matrix is the amide I (1,665 cm^{-1}), which largely arises from collagen [13, 14].

Post-creatine supplementation

Figure 4 shows the mean Raman spectra of the cortical and trabecular bones of all experimental groups as well as the mean integrated intensities of each Raman band. In the cortical bone, a slight increase in the Raman peak of the organic matrix content (1,665 cm^{-1}: amide I) can be observed in the OVX and CRE groups (Fig. 4a). However, ANOVA statistical analysis of the integrated intensities of the Raman bands showed no significant difference between the groups ($p>0.05$) (Fig. 4b). In the trabecular bone, the osteoporotic animals who did not receive Cr supplements (OVX) showed a lower intensity in the Raman markers of mineral content (phosphate and carbonate bands) (Fig. 4c). These results were statistically significant ($p<0.05$) when compared to the control group (SHAM). In addition, the supplemented animals (CRE) showed a significant increase in intensity of the main Raman marker of mineral content (959 cm^{-1}: phosphate) when compared to animals without supplementation (OVX) ($p<0.05$) (Fig. 4c and d).

Bone quality parameters

Table 1 presents the ratios used to determine bone quality for the cortical and trabecular bones. The cortical bone site revealed a statistically significant higher phosphate-amide I ratio in the OVX group compared to the SHAM group ($p<0.05$). Regarding the trabecular site, a statistically significant lower phosphate-amide I ratio in the OVX group was observed compared to the other two experimental groups (SHAM and CRE) ($p<0.05$). Although not significant ($p>0.05$), the bones from Cr-supplemented animals demonstrated an intermediate carbonate-phosphate ratio, which was higher than that for the osteoporotic animals without supplementation. There was no statistically significant difference in the carbonate-amide I ratios between the experimental groups ($p>0.05$). However, the trabecular bone site was generally associated with lower ratios when compared to the cortical bone site.

Raman findings and BMD correlations

Comparisons were also made between the findings obtained by the radiographic assessment of bone density and the Raman intensity of the main bone mineral marker (phosphate band, 959 cm^{-1}) using data from the cortical and trabecular bones for all experimental groups (Fig. 5). The Pearson's correlation coefficient revealed a high correlation for both cortical bones ($r^2=0.8037$) and trabecular sites ($r^2=0.9515$). It was noted that the cortical bone sites were more likely to have higher BMD values than the trabecular bone sites.

Discussion

Considering that osteoporosis is a very widespread disease that affects elderly people around the world, there is a great need to better understand the pathogenesis of this disease and to investigate new techniques for the diagnosis and therapy of osteoporotic bone. The purpose of this study was to examine the influence of Cr supplementation on bone quality from ovariectomized rats, a well-established model for experimental osteoporosis, using FT-Raman spectroscopy.

The key finding from the current study was that Cr supplementation in ovariectomized rats resulted in a significant increase in mineral contents of the lumbar vertebrae compared to ovariectomized rats without Cr supplementation. Emerging evidence suggests that Cr supplementation has the potential to influence bone biology [7, 32–36]. In fact, the presence of CK isoforms in bone and cartilage during different stages of development corroborates this hypothesis [26]. Similarly, it has been noted that chondrocyte hypertrophy is related to CK overexpression. In addition, Funanage et al. [33] showed that ß-guanidinopropionic acid administration (a Cr analog that competes for Cr uptake in the cells), which results in

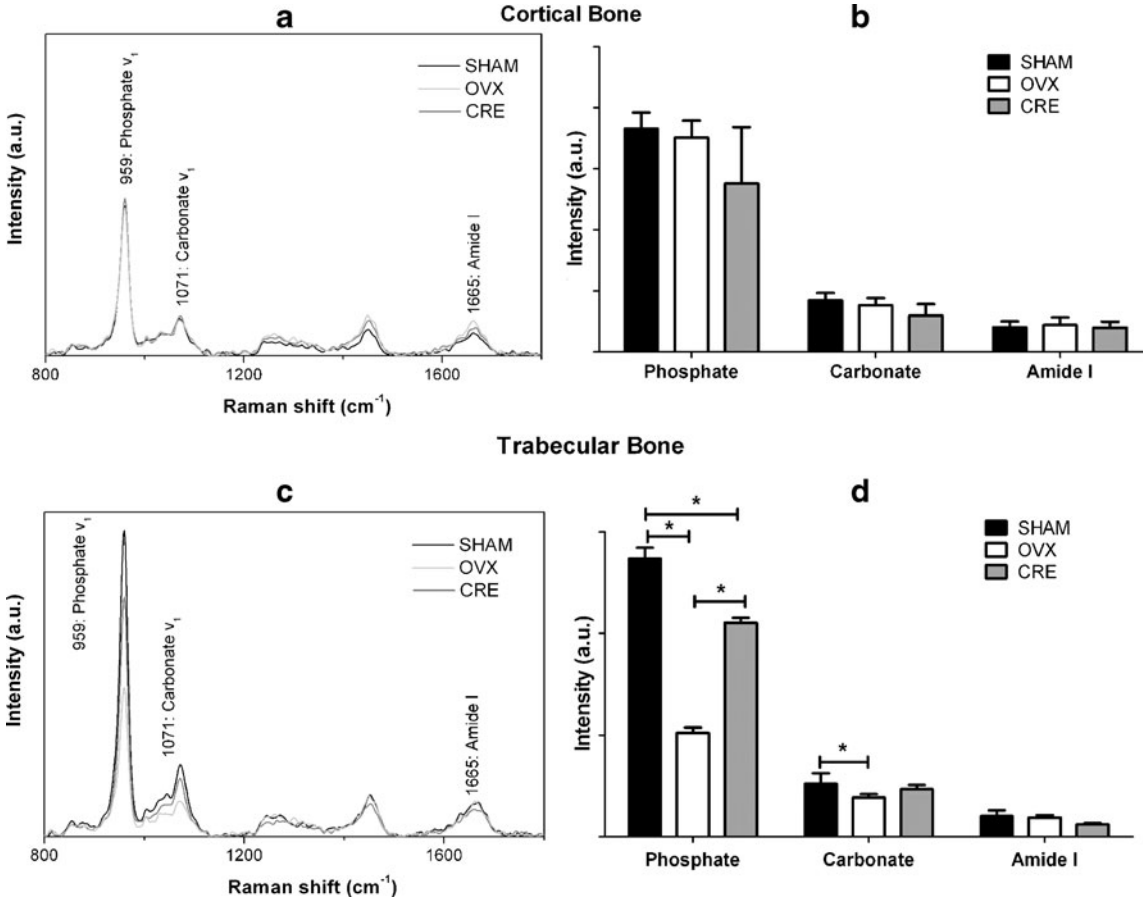

Fig. 4 Mean FT-Raman spectra and integrated intensities of Raman peaks on the cortical and trabecular bone sites from the OVX, CRE, and SHAM groups (n=7 per group); *a.u.* arbitrary units, *indicates a group with a statistically significant difference (p<0.05)

severe Cr content reductions, and consequently in disturbances in the CK system, provokes endochondral disorders in vitro and in vivo. In humans, observations revealed increased BMD in young boys diagnosed with Duchenne and Becker muscular dystrophy under chronic corticoid treatment (a drug that reduces BMD) when supplementation of Cr was furnished for 3 and 4 months, respectively. The effect of Cr seemed to involve a reduction in bone breakdown, since reduced urinary N-telopeptide excretion was observed [7, 34]. Using an animal model, Antolic et al. [35] studied the influence of Cr supplementation on bone structure and function in growing rats for 8 weeks in order to establish a therapeutic model by assessing the BMD using DXA at the beginning and end of the protocol. It was shown that the Cr-treated rats presented a greater lumbar BMD compared to the control rats. Recently, a stimulatory effect of Cr supplementation on metabolic activity, differentiation, and mineralization in rat osteoblast-like cells in culture was observed [31]. In fact, these effects were shown to be mediated by the direct action of the Cr-CK system on bone bioenergetics. Likewise, it is tempting to speculate on whether Cr supplementation could be used as an adjuvant therapy for aging bone healing as well as osteoporosis.

Research investigating the effects of Cr supplementation on aging bone is limited. Some studies investigated the effects of Cr supplementation combined with resistance training on BMD values in older men by using DXA [8–10]. The results showed that the Cr-supplemented group had increased BMD values compared to the placebo group. It was speculated that this increase in BMD might be due to an enhanced muscle mass after Cr supplementation, generating potentially greater tension at the sites of muscle attachment to bone. However, the effects of Cr supplementation on the mineralization process and bone microarchitecture at the molecular level in osteoporosis are unclear [4].

Currently, DXA is the gold standard screening model for diagnosing osteoporosis in humans: it identifies the risk of fracture by determining BMD. However, this technique is not capable of fully predicting bone strength because it cannot measure the bone microarchitecture and crystal organization or the structure of bone proteins. In fact, bone tissue is metabolically active and innumerous interactions

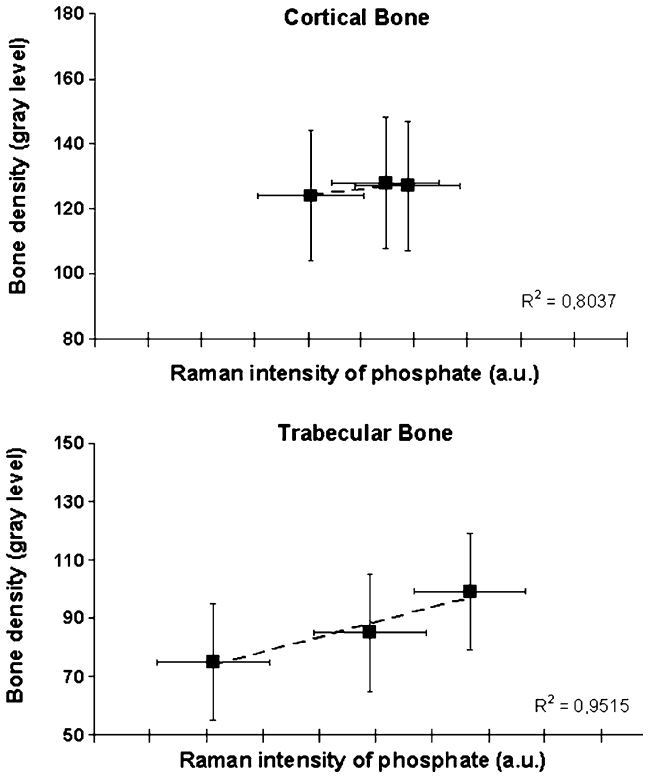

Fig. 5 Correlation between the radiographic assessment of BMD and the Raman intensity of the phosphate band (959 cm^{-1}) at cortical and trabecular bones sites; *a.u.* arbitrary units

between ions from the extracellular fluid and ions that constitute the apatite crystals and organic compounds are possible [37]. Thus, in the present study, the Raman technique was selected because it has the capability of nondestructively accessing the molecular structure of mineral and organic bone components, allowing a study of the properties of each individual component, as well as mineral–matrix interactions [13, 14]. Since the intensities of peaks are proportional to the relative amounts of the related species in vibrational spectroscopy [38], all of the major intensities of Raman bone peaks were selected to compare the degree of relative mineral and matrix contents between the normal and osteoporotic bones. Thus, a higher intensity represents a higher concentration of mineral or matrix contents.

In a previous study, an ovariectomized rat model of osteoporosis was studied using FT-Raman spectroscopy on the surface of site-specific bones (trabecular and cortical sites) [24]. It was possible to demonstrate that the Raman spectra of all bone sites clearly showed differences in the prominent vibrational bands related to bone biomarkers, such as phosphate, carbonate apatites, and collagen (959, 1,071 and 1,665 cm^{-1}, respectively). As occurred in the present study, FT-Raman spectroscopy showed a decreased level of mineral contents present in the trabecular bone sites from the OVX animals compared to the SHAM animals and, for the cortical bone sites, the mineral content was greater when compared to the other bone sites, independent of the experimental group. These differences were found between the bone sites were because not all bone sites in the ovariectomized rat exhibit such bone loss, nor did all the bone sites lose bone at the same rate [39]. For instance, the earliest significant trabecular bone loss in the femoral neck and lumbar vertebrae occurred at 30 and 60 days, respectively. In contrast, ovariectomy-induced bone loss did not occur in the cortical bone site [40].

In spite of a reduction in the mineral content of trabecular bone observed through the BMD of OXV rats in previous studies [18, 41–43], the reduction in intensity of the main Raman peak of bone mineral content (the phosphate band at 959 cm^{-1}) after ovariectomy in the trabecular bone site only, as observed in this study, indicates the monitoring ability of bone changes by FT-Raman spectroscopy and suggests the effectiveness of ovariectomy. In the present study, only the phosphate band at 959 cm^{-1} was used to assess the bone mineral contents because other Raman phosphate vibrations (431, 589, and 1,044 cm^{-1}) are associated with labile and non-apatitic phosphate species in immature bone and indicate the possible existence of bone precursors that ovariectomy does not appear to directly affect [13, 14]. Using other animal models to induce osteoporosis, Shen et al. [44] and Apeldoorn et al. [45] also demonstrated a severe decrease in the intensity of the main phosphate apatite Raman band compared to the control group.

In contrast, ovariectomy-induced mineral bone loss did not occur in cortical bone (Fig. 4a and b). It was shown that OVX stimulates periosteal bone growth in the cortical bone diaphysis, and that an increase in bone resorption only affects the endosteum [46]. Although not significant, this study showed that the cortical bone of the OVX group had a higher intensity of the Raman peak related to the collagen matrix (amide I: 1,665 cm^{-1}). It is possible that ovariectomy-induced periosteal bone growth may influence osteoblastic production of the extracellular matrix, and the major component of this unmineralized matrix is type I collagen [47]. Thus, the Raman peak of amide I, which largely arises from bone collagen, could adequately illustrate this variation.

In order to study bone quality phenomena, the ratios between phosphate-amide I (959/1,665 cm^{-1}), carbonate-phosphate (1,071/959 cm^{-1}), and carbonate-amide I (1,071/1,665 cm^{-1}) were used, as in previous studies [26–29]. A lower phosphate-amide I ratio was observed in cortical and trabecular bones from the OVX group ($p<0.05$). The similarity in the results for both bones must be contrasted the following way: in the case of trabecular bone, ovariectomy caused a reduction in the mineral content and

the resulting reduction in the mineral-to-matrix ratio was directly proportional. In the case of cortical bone, ovariectomy did not reduce the mineral content but instead it increased the Raman peak of amide I, so this reduction in the mineral-to-matrix ratio was inversely related. In addition, the values obtained for the phosphate-amide I ratio in the CRE group were higher than in the OVX group. Thus, the trend towards the decreased mineral-matrix ratio as seen here suggests the possibility that osteoporosis was a result of chemical changes in the bone. Because the phosphate-amide I ratio indicates the amount of mineralization [26], Cr supplementation could have had a beneficial effect on osteoporotic bone tissue as result of higher phosphate-amide I ratio than in rats without supplementation.

A difference in the carbonate-phosphate ratio may indicate bone architecture, age, and mineral crystallinity differences in the bone tissues and appears to be a key variable in osteoporotic fractures [27–29]. McCreadie et al. [26] observed a greater carbonate-phosphate ratio in iliac crest cortical bone from women with fractures. Using infrared microspectroscopy, Gadeleta et al. [48] showed that the mineral crystals in both OVX monkeys and osteoporotic humans were larger, more crystalline, and had a greater carbonate-phosphate ratio than bone from controls and non-osteoporotic humans. In agreement with these studies, the values of the carbonate-phosphate ratio presented here were also higher in the OVX group, especially in cortical bone. Thus, Cr supplementation also positively influenced this Raman ratio. The peak at 1,071 cm^{-1} was used, which is formed by the primary carbonate vibrational mode and indicates the extent of carbonate incorporation in the hydroxyapatite lattice (type-B carbonate substitution), due to its association with agin [49]. It is probable that in ovariectomized animals there is a greater selective resorption of older, more mature bone mineral, which contains a higher concentration of carbonate than young bone [50]. In fact, the process of osteoporosis seems to involve advanced bone that could be considered as immature but older [13, 14].

Although the carbonate/amide I ratio can indicate bone remodeling [26], little attention has been paid to this ratio. In the present study, it was shown that the cortical bone site had greater values compared to the trabecular bone site in the same experimental group (Fig. 5). This difference is consistent with the cortical bone appearing to be "older" than trabecular bone because of its slower turnover rate, a finding consistent with the lower turnover of bone observed in the cortical compartment.

Because of the extensive variation between the various bone sites and bone types, experimental methods that yield highly comprehensive information with minimal difficulty are desirable. Vibrational spectroscopy is an extremely useful tool in this endeavor. In this sense, it is important to note that the results of the measurements of the radiographic assessment of bone density were encouraging as the same findings were shown by Raman intensity of phosphate from cortical (r^2=0.8037) and trabecular bones (r^2=0.915).

In summary, both bone phases (the mineral and organic matrices), in addition to the mineral bone quantity, as measured by DXA, were considered important for understanding how Cr supplementation could act in cortical and trabecular bones from rats with OVX-induced osteoporosis. The present study demonstrates that Raman spectroscopy could be a feasible method for the non-destructive assessment of bone tissue composition, particularly the amounts and ratio of the mineral and matrix phases, either alone or in conjunction with bone density evaluations. With the advance of fiber optic Raman spectroscopy, optimization of this technique will be possible, allowing the detection of more subtle differences in specific spectral features. Furthermore, the results of the present study provide additional support to the theory that the chemical composition of bone tissue may be positively influenced by Cr supplementation after ovariectomy.

Acknowledgments R.A. Souza thanks FAPEMIG (Fundação de Amparo a Pesquisa do Estado de Minas Gerais) for the research grant support (APQ-02900-10). L. Silveira Jr. thanks CNPq (Conselho Nacional de Desenvolvimento Científico e Tecnológico) for the Productivity Fellowship (305610/2008-2).

References

1. Wyss M, Kaddurah-Daouk R (2000) Creatine and creatinine metabolism. Physiol Rev 80(3):1107–1213
2. Walker JB (1979) Creatine biosynthesis, regulation and function. Adv Enzymol Relat Area Mol Biol 50:117–242
3. Bemben MG, Lamont HS (2005) Creatine supplementation and exercise performance: recent findings. Sports Med 35 (2):107–125
4. Gualano B, Artioli GG, Poortmans JR, Lancha Junior AH (2010) Exploring the therapeutic role of creatine supplementation. Amino Acid 38(1):31–44
5. Raisz LG (2005) Pathogenesis of osteoporosis: concepts, conflicts, and prospects. J Clin Invest 115(12):3318–3325
6. Johnell O, Kanis J (2005) Epidemiology of osteoporotic fractures. Osteoporos Int 16(Suppl 2):S3–S7
7. Louis M, Lebacq J, Poortmans JR, Belpaire-Dethiou MC, Devogelaer JP, Van Hecke P, Goubel F, Francaux M (2003) Beneficial effects of creatine supplementation in dystrophic patients. Muscle Nerve 27(5):604–610
8. Chilibeck PD, Chrusch MJ, Chad KE, Shawn Davison K, Burke DG (2005) Creatine monohydrate and resistance training increase bone mineral content and density in older men. J Nutr Health Aging 9(5):352–353
9. Candow DG, Chilibeck PD (2007) Effect of creatine supplementation during resistance training on muscle accretion in the elderly. J Nutr Health Aging 11(2):185–188
10. Candow DG, Chilibeck PD (2010) Potential of creatine supplementation for improving aging bone health. J Nutr Health Aging 14(2):149–153

11. Boivin G, Meunier PJ (2003) The mineralization of bone tissue: a forgotten dimension in osteoporosis research. Osteoporos Int 14 (Suppl3):S19–S24
12. Ammann P, Rizzoli R (2003) Bone strength and its determinants. Osteoporos Int 14(Suppl 3):S13–S18
13. Carden A, Morris MD (2000) Application of vibrational spectroscopy to the study of mineralized tissues (review). J Biomed Optics 5(3):259–268
14. Morris MD, Mandair GS (2010) Raman assessment of bone quality. Clin Orthop Relat Res Nov 30 [Epub ahead of print]
15. Judex S, Boyd S, Qin Y-X, Miller L, Muller R, Rubin C (2003) Combining high-resolution micro-computed tomography with material composition to define the quality of bone tissue. Curr Osteoporos Rep 1(1):11–19
16. Hanlon EB, Manoharan R, Koo TW, Shafer KE, Motz JT, Fitzmaurice M, Kramer JR, Itzkan I, Dasari RR, Feld MS (2000) Prospects for in vivo Raman spectroscopy. Phys Med Biol 45(2):R1–R59
17. Moreira LM, Silveira L Jr, Santos FV, Lyon JP, Rocha R, Zângaro RA, Villaverde AB, Pacheco MTT (2008) Raman spectroscopy: a powerful technique for biochemical analysis and diagnosis. Spectrosc Int J 22(1):1–19
18. Kalu DN (1991) The ovariectomized rat as a model of postmenopausal osteopenia. Bone Miner 15:175–191
19. Brannon TA, Adams GR, Conniff CL, Baldwin KM (1997) Effects of creatine loading and training on running performance and biochemical properties of rat skeletal muscle. Med Sci Sports Exerc 29(4):489–495
20. Gagnon M, Maguire M, MacDermott M, Bradford A (2002) Effects of creatine loading and depletion on rat skeletal muscle contraction. Clin Exp Pharmacol Physiol 29(10):885–890
21. McGuire M, Bradford A, MacDermott M (2002) Contractile properties of the diaphragm in creatine-fed rats. Clin Experim Pharm Physiol 29(9):782–783
22. Greenhaff PL, Bodin K, Soderlund K, Hultman E (1994) The effect of oral creatine supplementation on skeletal muscle phosphocreatine resynthesis. Am J Physiol 266(5 Pt 1):E725–E730
23. Hultman E, Soderlund K, Timmons JA, Cederblad G, Greenhaff PL (1996) Muscle creatine loading in men. J Appl Physiol 81 (1):232–237
24. Souza RA, Jeronimo DP, Gouvea HA, Xavier M, Souza MT, Miranda H, Tosato MG, Martin AA, Ribeiro W (2010) Fourier-transform Raman spectroscopy study of the ovariectomized rat model of osteoporosis. Open Bone J 2(1):24–31
25. Da Silva FF, Souza RA, Pacheco MT, Ribeiro W, da Silva MA, Miranda H, Salgado MA, de Melo Castilho JC, Silveira L (2011) Effects of different swimming exercise intensities on bone tissue composition in mice: a Raman spectroscopy study. Photomed Laser Surg 29(4):217–225
26. McCreadie BR, Morris MD, Sudhaker CTC, Rao D, Finney WF, Widjaja E, Goldstein SA (2006) Bone tissue compositional differences in women with and without osteoporotic fracture. Bone 39:1190–1195
27. Ager JW, Nalla RK, Breeden KL, Ritchie RO (2005) Deep-ultraviolet Raman spectroscopy study of the effect of aging on human cortical bone. J Biomed Opt 10:034012
28. Legros R, Balmain N, Bonel G (1987) Age-related changes in mineral of rat and bovine cortical bone. Calcif Tissue Int 41:137–144
29. Yerramshetty JS, Lind C, Akkus O (2006) The compositional and physicochemical homogeneity of male femoral cortex increases after the sixth decade. Bone 39:1236–1243
30. Martins MV, da Silva MA, Medici Filho E, de Moraes LC, Castilho JC, Da Rocha RF (2005) Evaluation of digital optical density of bone repair in rats medicated with ketoprofen. Braz Dent J 16:207–212
31. Sakakura CE, Giro G, Gonçalves D, Pereira RM, Orrico SR, Marcantonio E Jr (2006) Radiographic assessment of bone density around integrated titanium implants after ovariectomy in rats. Clin Oral Implants Res 17:134–138
32. Wallimann T, Hemmer W (1994) Creatine kinase in non-muscle tissues and cells. Mol Cell Biochem 133:193–220
33. Funanage VL, Carango P, Shapiro IM, Tokuoka T, Tuan RS (1992) Creatine kinase activity is required for mineral deposition and matrix synthesis in endochondral growth cartilage. Bone Miner 17:228–236
34. Tarnopolsky MA, Mahoney DJ, Vajsar J, Rodriguez C, Doherty TJ, Roy BD, Biggar D (2004) Creatine monohydrate enhances strength and body composition in Duchenne muscular dystrophy. Neurology 62:1771–1777
35. Antolic A, Roy BD, Tarnopolsky MA, Zernicke RF, Wohl GR, Shaughnessy SG, Bourgeois JM (2007) Creatine monohydrate increases bone mineral density in young Sprague-Dawley rats. Med Sci Sports Exerc 39:816–820
36. Gerber I, ap Gwynn I, Alini M, Wallimann T (2005) Stimulatory effects of creatine on metabolic activity, differentiation and mineralization of primary osteoblast-like cells in monolayer and micromass cell cultures. Eur Cell Mater 10:8–22
37. Mundy GR (1999) Cellular and molecular regulation of bone turnover. Bone 24:35–38
38. Goodyear SR, Gibson IR, Skakle JMS, Wells RPK, Aspden RM (2009) A comparison of cortical and trabecular bone from C57 black 6 mice using Raman spectroscopy. Bone 44:899–907
39. Jee WSS, Yao W (2001) Overview: animal models of osteopenia and osteoporosis. J Musculoskel Neuron Interact 1:193–207
40. Wronski TJ, Cintron M, Dann LM (1988) Temporal relationship between bone loss and increased bone turnover in ovariectomized rats. Calcif Tissue Int 42:179–183
41. Braun MJ, Reiners C, Schiel H, Allolio B (1996) Changes in biomechanical properties of rat femora induced by ovariectomy as analyzed by pQCT. Osteoporos Int 6:194
42. Sheng ZF, Dai RC, Wu XP, Fang LN, Fan HJ, Liao EY (2007) Regionally specific compensation for bone loss in the tibial trabeculae of estrogen-deficient rats. Acta Radiol 48:531–539
43. Pajamäki I, Sievänen H, Kannus P, Jokihaara J, Vuohelainen T, Järvinen TL (2008) Skeletal effects of estrogen and mechanical loading are structurally distinct. Bone 43:748–757
44. Shen J, Fan L, Yang J, Shen AG, Hu JM (2010) A longitudinal Raman microspectroscopic study of osteoporosis induced by spinal cord injury. Osteoporos Int 21:81–87
45. Van Apeldoorn AA, De Boer J, Van Steeg H, Hoeijmakers JHJ, Otto C, Van Blitterswijk CA (2007) Physicochemical composition of osteoporotic bone in the trichothiodystrophy premature aging mouse determined by confocal Raman microscopy. J Gerontol A Biol Sci Med Sci 62:34–40
46. Turner RT, Maran A, Lotinun S, Hefferan RT, Evans GL, Zhang M, Sibonga JD (2001) Animal models for osteoporosis. Rev Endocr Metab Disord 2:117–127
47. Matsuo K, Irie N (2008) Osteoclast-osteoblast communication. Arch Biochem Biophys 473:201–209
48. Gadeleta SJ, Boskey AL, Paschalis E, Carlson C, Menschik F, Baldini TA (2000) Physical, chemical, and mechanical study of lumbar vertebrae from normal, ovariectomized and nandrolone decanoate-treated cynomolgus monkeys (Macaca fasciculares). Bone 27:541–550
49. Akkus O, Adar F, Schaffler MB (2004) Age-related changes in physicochemical properties of mineral crystals are related to impaired mechanical function of cortical bone. Bone 34:443–453
50. Bohic S, Rey C, Legrand A, Sfihi H, Rohanizadeh R, Martel C, Barbier A, Daculsi G (2000) Characterization of the trabecular rat bone mineral: effect of ovariectomy and bisphosphonate treatment. Bone 26:341–348